Suppressing Turbulence Induced Vibration of the Head Suspension Assembly in a Hard Disk Drive

Byoung-Cheol Kim
Dynamic Stability Laboratory
1113 Etcheverry Hall
University of California
Berkeley, CA94720
e-mail:bckim@mote.me.berkeley.edu

C. D. Mote, Jr.
Glenn L. Martin Institute
Professor of Engineering and President
University of Maryland
College Park, MD20742
e-mail: dmote@deans.umd.edu

Abstract

Higher read/write density and faster data transfer rates in hard disk drive are continuous in a demand. As the disk speed increases, airflow induced vibration becomes a principal obstacle to achievement of higher track densities. In this work, flow fluctuations were measured upstream of the load beam and slider with a constant temperature hot wire anemometer. Radial displacement of the slider was measured with a laser Doppler displacement meter. The mean and fluctuating components of the air velocity near the head suspension assembly are compared to the slider motion under changes with cover geometry. Slider vibration in the first torsional mode of head suspension assembly, which is a principal contribution to track misregistration, was reduced with a modification of cover geometry.

1 Introduction

Market demands push the design of computer hard disk drives (HDD) towards higher storage capacities, faster data transfer rates and higher reliability. The data storage capacity of a HDD can be increased with higher track density (tracks per inch, TPI) and higher bit density (bits per inch, BPI). The track density of current commercial magnetic disk drives exceeds 10,000 TPI and is projected to exceed 25,000 TPI by the turn of the century. Track misregistration (TMR) by the head must be essentially eliminated in order to achieve these very high track densities. The requirements for accurate positioning of the head become a more challenging as TPI increases. Higher disk rotation speed is also always in demand to increase data transfer rates. However, increased disk speed increases the aerodynamic forces that induce the vibration of head suspension assembly coupled to the airflow. Accordingly the flow induced vibration of the head suspension assembly degrades data transfer reliability.

The influence of air flow in a hard disk drive on the suspension vibration was first investigated by Yamaguchi *et al*. (1986). They found that the vibration amplitude of the suspension was proportional to the square of the approaching velocity. In their subsequent studies (Yamaguchi *et al*., 1990, Tokuyama *et al*., 1991), flow fluctuation in the wake of the suspension was measured by hot wire anemometer to examine the effect of the air flow on suspension vibration. These papers indicated that the suspension vibrates at its natural frequencies even though the spectrum of flow pressure has dominant peak at different frequencies and the flying height fluctuation can be reduced by using aerofoil type suspension. Although they observed that the instability induced vibration (caused by vortex shedding) of suspension is negligible, extraneously induced vibration (caused by turbulence) was not studied. Harrison *et al* (1993) studied the air flow between a pair of corotating disks using a hot wire anemometer. Mean and rms flow velocity were measured using a hot wire probe at the tip of an obstruction in order to simulate the flow profile as viewed by a head suspension assembly in a hard disk drive. They observed that rms amplitude of flow fluctuation generally increases as the radial position of hot wire tip increases. They also found that local maxima in rms flow

fluctuation exist. Although their work contributed to the understanding of flow characteristics in corotating disks and supported previous results by Lennemann, (1974), Abrahamson *et al*., (1989), Usry *et al.*, (1990), Tzeng *et al*., (1990,1991), Humphrey *et al*., (1991) and Schuler *et al*., (1991), the effect of turbulent air flow in HDD on the vibration of head suspension assembly was not measured.

The objectives in this work is to find the effect of turbulent flow in a HDD on the torsional mode of head suspension assembly with the changes of disk speed and slider location and to alter the turbulence induced vibration by modifying the air flow through change in the cover geometry.

2 Slider vibration in the first torsional mode of HGA

The head suspension assembly, also known as the head gimbal assembly (HGA) consists of a slider, load beam, flexure and base plate (see Fig. 1). As the vibration modes of the HGA modes are excited by the flow around it, the most critical modes are the ones which causes the head to deviate from a desired track. This is called off-track motion or track misregistration. Typically the torsional modes and the lateral bending (sway) modes cause the off-track motion. This work addresses vibration in the first torsional mode of HGA.

The vibration of the slider in the radial direction of the top disk was measured using a Laser Doppler Displacement Meter (LDDM). A typical power spectrum of the slider vibration (the radial distance from the disk center to the slider, R_s = 32 mm, disk speed = 11,100 rpm) is shown in Fig. 2.

The slider vibration of large magnitude at lower frequencies in Fig. 2 (typically less than 350Hz for 5400 rpm disk drives) can be controlled through the servo system and feedforward cancellation. Thus, vibration in this band is not of our principal concern. A dominant vibration amplitude peak appeared at 2.64 kHz. The area under this peak is a measure of their contribution to track misregistration (TMR). This work will show that this peak is caused by a vibration mode of HGA that is excited by turbulent fluid flow. With the spectrum displayed in power spectral density units, when converted into displacement, the total area under the curve represents the variance σ^2 of the slider

vibration. In a Gaussian distribution, the maximum vibration amplitude is estimated to be 3σ. A peak in the radial slider vibration spectrum increases with the disk speed as shown in Fig. 3. The peak at 2.64 kHz grows significantly in magnitude as disk speed increases. In order to find a measure of the contribution of this peak to the variance of the slider vibration, the term $\hat{s}$ is defined as follows:

$$\begin{aligned} s^2 &= \int_0^\infty S_{xx}(f)df = \int_0^{f_1} S_{xx}(f)df + \int_{f_1}^{f_2} S_{xx}(f)df + \int_{f_2}^\infty S_{xx}(f)df \\ &= s_1^2 + s_2^2 + s_3^2 \end{aligned} \tag{1}$$

$$\hat{s} = 3s_2 = 3\sqrt{\int_{f_1}^{f_2} S_{xx}(f)df} \tag{2}$$

with f_1 and f_2 are 2550, 2750 Hz respectively and $S_{xx}(f)$ is the power spectral density function.

The radial slider vibrations were measured at 11 positions of the slider (from 22mm to 42 mm) from the disk center and at 20 disk speeds from 5,400 rpm to 11,100 rpm. $\hat{s}$, calculated from these vibration data, are shown in Fig. 4. $\hat{s}$ increases with disk speed at speeds exceeding 8,000 rpm. They tend to increase also with the radial positions of the slider though local maxima is seen at 28 mm.

3 Experimental modal analysis of Head Gimbal Assembly

The peak amplitude of vibration at 2.64 kHz was found to represent the first torsional vibration mode of the HGA. This was confirmed by modal analysis of the HGA. The schematic of experimental setup for modal analysis is shown in Fig. 5. The current to the voice coil motor (VCM) was the input of Frequency Response Function and the vibration signal from the lateral slider vibration / vertical suspension vibration was the output. The vertical vibration of the suspension was measured at 27 points. The magnitude and phase in FRF data from slider / suspension were used to obtain the natural frequency and mode shape. To ensure identical air flow excitation to that in normal operation of the disk drive, the LDDM laser beam passed through a glass window with 99.7% transmissivity.

The head suspension assembly was excited by applying a white noise voltage to voice coil motor.

The measured frequency response of the radial displacement of slider is shown in Fig. 6(a). A peak amplitude from the first torsional mode of HGA was found at 2.64 kHz and a system mode was found at around 3.78 kHz. The system mode is known to couple the vibration of the head, suspension, arm and ball bearing assembly. Control of this system mode by use of a passive vibration damper was recently proposed by Jiang and Miles (1999). The magnitudes from measured frequency response of the vertical displacement of load beam at 3 different positions are shown in Fig. 6(b,c,d). The peak at the same frequency (2.64 kHz) was found. Also shown are the peaks from bending mode of load beam. The measured mode shape of the first torsional mode of head suspension assembly is shown in Fig. 6(e).

4 Turbulence induced vibration : theoretical background

A review of turbulence induced vibration is well presented by Blevins (1990) and Naudascher (1994). The response of a structure to the excitation by turbulent flow is considered in two parts. The first concerns prediction of the loading on the structure from the mean and fluctuating components of the flow. The second addresses the prediction of the structural response from the loading and structural characteristics. The problem of relating the velocity fluctuations to the pressure and force fluctuation on a bluff body in turbulent flow can be simplified by assuming that the instantaneous load, dF , acting on an incremental area, dA, is related to the instantaneous velocity incident on that area in the form (Vickery & Davenport, 1967)

$$\frac{dF}{dA} = C_D \frac{r v^2}{2} + C_m r \frac{\partial v}{\partial t} \tag{3}$$

where C_D and C_m are the equivalent drag and inertia coefficients. If the inertia force component $C_m r \partial v / \partial t$ and the term $(v'/\bar{v})^2$ are assumed relatively negligible and v and F are expressed in terms of their mean and fluctuating components,

$$v = \bar{v} + v' \qquad F = \overline{F} + F' \tag{4}$$

Equation (3) simplifies to the quasi-steady simplification:

$$dF \cong C_D \frac{r\bar{v}^2}{2} dA, \qquad dF' \cong C_D r\bar{v}v' dA \tag{5}$$

To describe the frequency content of the fluctuations in velocity v', pressure p' and drag F', we employ the power spectral densities

$$S_v(f) = \frac{\overline{v_f'^2}}{df}, \quad S_p(f) = \frac{\overline{p_f'^2}}{df}, \quad S_F(f) = \frac{\overline{F_f'^2}}{df}, \tag{6}$$

where $\overline{v_f'^2}$, $\overline{p_f'^2}$ and $\overline{F_f'^2}$ are mean square values that lie within a frequency band *df* centered around *f*. The cospectral density of the velocity fluctuations v_1' and v_2' on two incremental areas dA_1 and dA_2

$$S_{12}(f) = \frac{\overline{[v_1'v_2']}_f}{df}, \tag{7}$$

is the time average of that part of the normalized product $v_1'v_2'$ that is associated with the frequency *f*. An approximation of the rms value of the fluctuating force acting on the structure can be written as (Naudascher, 1994) :

$$F'_{rms} = \sqrt{\overline{F'^2}} \cong C_D r\bar{v}\sqrt{\overline{v'^2}} \left(\iint \frac{\overline{v_1'v_2'}}{\overline{v'^2}} dA_1 dA_2 \right)^{1/2} \tag{8}$$

When an expression for F_f' from equations (5), (7) and (8) is substituted in equation (6) along with $\bar{F} = C_D A\bar{v}^2/2$, one obtains

$$S_F(f) = 4\left(\frac{\bar{F}}{\bar{v}}\right)^2 \left|c_{fl}(f)\right|^2 S_v(f) \tag{9}$$

with $$\left|c_{fl}(f)\right|^2 = \frac{1}{A^2} \iint \frac{S_{12}(f)}{S_v(f)} dA_1 dA_2 \tag{10}$$

Here, $c_{fl}(f)$ is the fluid-dynamic admittance (Vickery & Davenport, 1967), which depends on the geometry of the bluff body. For a circular cylinder of length L, $c_{fl}(f)$ in equation (9) can be replaced by $\left|J_i(f)\right| \Big/ \int_0^L \tilde{y}_i(z)dz$, where $J_i(f)$ is the joint acceptance (Chen & Wambsganns, 1972) and $\tilde{y}_i(z)$ is the mode shape along the axis *z* of the body.

In $J_i(f)$, the correlation between deflections *y* is also taken into account (Naudascher, 1994):

$$\left|J_i(f)\right|^2 = \frac{1}{A^2}\iint\left[\tilde{y}_i(z_1)\tilde{y}_i(z_2)\frac{S_{12}(f)}{S_v(f)}\right]dA_1\,dA_2 \tag{11}$$

The joint acceptance of a mode is a measure of the efficiency of the excitation of the mode by the velocity. The joint acceptance of a simply-supported cylinder in axial turbulent flow was studied earlier by Chen *et al.* (1972) and Blevins (1990). From equation (9), $S_F(f) \approx \bar{v}^2 \cdot S_v(f)$ shows that the system response for the fluid dynamic loading is approximately proportional to $\bar{v} \cdot v'$. In this experimental analysis, the turbulence induced vibration of HGA is predicted by measuring the mean and fluctuating part of the velocity near the HGA.

5 Turbulence induced vibration of HGA : experiment

5.1 Experimental setup for measurement of flow near HGA

To investigate the source of excitation of the first torsional mode of the HGA, the flow fluctuations near the load beam and the slider were measured. A single, constant temperature tungsten hot wire sensor of diameter 0.0038mm and sensor length 1.25mm was used for the measurement. To measure the flow near the load beam and slider within the cover, the hot wire was inserted into the gap between the disk surface and bottom surface of the cover through 2x2 mm hole on the cover. The mean and fluctuating air velocities were measured at 5 locations from the disk surface near the load beam and the slider. Hot wire locations for measuring the flow upstream of load beam and slider are shown in Fig. 7. The hot wire was placed precisely in the radial and tangential positions (r, θ,z) by using x-y stages and micrometer stage as shown in Fig. 8.

5.2 Effect of cover geometry on the turbulent flow near HGA

To examine the effect of the cover geometry on the turbulent flow around the head suspension assembly, two solid blocks were attached to the bottom surface of the cover as shown in Fig. 9 (a),(b). The block was placed upstream of the HGA for cover 1 and downstream of the HGA for cover 2. Then the hot wire measurement was repeated with and without these two covers. The blocks that were used in cover 1 and cover 2 are designed to block the air flow in the gap between the disk and cover by 77% (see Fig. 9(c)).

Typical power spectra with the conventional cover, cover 1, cover 2 and without a cover are shown in Fig. 10 (R_s = 32mm, disk speed = 11100 rpm). It is observed that turbulence in the uncovered test is higher than in the covered tests at the lower frequency ranges but is much lower in the higher frequency ranges. The flow fluctuation with cover 1 was higher than with conventional cover and with cover 2 in all the frequency ranges because the turbulent kinetic energy created by the block upstream of HGA was greater. The distributions of the streamwise velocity and turbulent kinetic energy in separated flow over a backward-facing step was studied by many researchers (Eaton *et al*. (1981), Neto *et al*. (1993), Kasagi *et al*. (1993,1995), Le *et al*. (1997)).

It was also observed in Fig. 10 that cover 2, which positions the block downstream of suspension assembly, reduces the turbulence near the load beam and slider. The variation of turbulence intensity with the changes of cover geometry demonstrates that the intensity of excitation by turbulent flow is strongly dependent on the cover geometry.

The results of hot wire measurement upstream of load beam in the different cover configuration is shown in Fig. 11. The fluctuating components of velocity in tangential and radial direction were averaged over the frequency range Δf (2550 ~ 2750 Hz) and were averaged again at the 5 different heights. Those values for 4 different cases are compared in (a.1), (b.1) at different disk speeds. The fluctuating component of velocity increases with the disk speed increase in all cases and the magnitudes in decreasing order are; cover 1, conventional cover, cover 2 and uncovered. It was found that v' in the uncovered case is negligibly small compared to those in the covered cases implying that the cover induces turbulent kinetic energy in the air between the disk surface and the cover. The mean velocities in tangential and radial direction were averaged over 5 different heights for each case and compared in (a.2) and (b.2). The order in the

magnitudes of mean velocities is different from that of fluctuating components of velocity. The mean velocity at each point was then multiplied by the fluctuating component of velocity at that point (averaged over Δf) and those values from 5 different heights were averaged. The averaged values for 4 different cases are compared in (a.3), (b.3). The magnitudes for each case and for the disk speed ((a.3), (b.3)) generally follow the same trends in (a.1) and (b.1). In tangential direction, there are differences in v' between conventional cover and cover 2 but the mean velocities with cover 2 are larger than those with conventional cover. So there are small differences in the magnitudes of $\bar{v} \cdot v'$ between the conventional cover and cover 2. However, the same differences of v' in the radial direction are magnified in $\bar{v} \cdot v'$ by the mean velocities, suggesting the possibility of reducing the dynamic loading on the load beam by using cover 2.

The same experiment was repeated upstream of slider at 5 different heights, in the tangential and radial directions, at 6 disk speeds between 5400 rpm and 11100 rpm. The results are shown in Fig. 12. Comparing with the results from upstream of load beam as shown in Fig. 11, in uncovered case, $\bar{v} \cdot v'$ upstream of slider is larger than that upstream of load beam. On the other hand, in covered cases, $\bar{v} \cdot v'$ of upstream of slider are smaller than those of upstream of load beam. The differences in v' and $\bar{v} \cdot v'$ between conventional cover and cover 2 in the radial direction can be also found upstream of slider (Fig. 12 (b.1) and (b.3)).

5.3 Effect of cover geometry on the slider vibration

To determine the influence of the cover geometry on the radial slider vibration near the first torsional mode vibration frequency of head suspension assembly, the slider motion was measured with cover 1, cover 2, the conventional cover and in the uncovered case. The slider vibration in the first torsional mode of HGA at different disk speeds and slider positions, 22 mm, 32 mm and 42 mm are compared in Fig. 13. It can be seen that slider vibration was aggravated under cover 1 and its effect when the slider is located at 42mm from the disk center is particularly large. However, with cover 2, $\hat{s}$ was reduced significantly, compared to conventional cover case at three slider positions. It is consistent with the results from hot wire measurements near HGA. It is observed that the

plot in Fig. 13(b) (R_s = 32 mm) is qualitatively similar to the trend shown in Fig. 11(b.3), when the 4 cases tested in this experiment are compared. Therefore, the fluid-dynamic loading in radial direction near the load beam has a strong correlation to the fluctuating component of slider motion in the first torsional mode of HGA.

Slider vibration in the first torsional mode of HGA, $\hat{s}$ with cover 2, when it is located at 11 positions from 22 mm to 42mm, is compared with those with conventional cover in Fig. 14. $\hat{s}$ was reduced at all slider positions tested at the higher disk speeds. It is concluded that blocking the flow downstream of HGA reduces mean and fluctuation component of the velocity, and hence decreases the turbulence excitation on the first torsional mode of HGA. The percentage reduction of $\hat{s}$ from the conventional cover to cover 2 with disk speeds are shown in Table 1. It is noted that positive effect of cover 2 increases as the disk spins faster, which suggests that using the idea behind cover 2 will have more effective control on the turbulence induced vibration for higher speed disk drives.

6 Conclusion

A dominant peak in the radial slider motion, that increases significantly with disk speed, was found. It was found to be the first torsional mode of HGA that was excited by turbulent air flow. Airflow near head suspension assembly in a hard disk drive was investigated by measuring the mean and fluctuation components of the velocity. The product of mean and fluctuating component of velocity near the load beam has strong correlation to the radial slider vibration. By changing the cover geometry, the slider vibration in the first torsional mode of HGA was significantly reduced especially at higher disk speeds where turbulent excitation is more significant.

References

[1] Abrahamson, S., Koga D.,and Eaton J., 1989, " The flow between corotating shrouded disks," Physics of Fluids A, Vol. 1, No. 2, pp. 241-251.

[2] Schuler, C., Usry, W.,Weber, B., Humphrey,J., and Greif, R., 1990,"On the flow in the unobstructed space between shrouded corotating disks," Physics of Fluids A, Vol. 2, No. 10, pp. 1760-1770.

[3]Abrahamson, S., Chiang, C., and Eaton, J., 1991. "Flow structure in head disk assemblies and implications for design," Adv. Info. Storage Syst., Vol. 1, pp. 111-132.

[4] Harrison, J. C.,Lou, D. H., Talke, F. E.,1993," Airflow at the tip of an obstruction between corotating disks," Adv. Info. Storage Syst., Vol. 5, pp. 159-174.

[5] Girard, J., Abrahamson, S., Uznanski, K., 1995,"The effect of rotary arms on corotating disk flow", Journal of Fluid Engineering, Vol. 117, pp. 259-262

[6] Suzuki, H., Humphrey,J.,1997,"Flow past large obstructions between corotating disks in fixed cylindrical enclosures," Journal of Fluid Engineering, Vol. 119, pp. 499-505

[7] Yamaguchi, Y., Talukder, A. A.,Shibuya, T., and Tokuyama, M., 1990, "Air flow around magnetic – head – slider suspension and its effect on slider flying – height fluctuation," IEEE Trans. Magn., Vol. 26, No, 5, pp. 2430-2432.

[8] Tokuyama, M., Yamaguchi, Y.,Miyata, S., and Kato, C., 1991, "Numerical analysis of flying height fluctuation and positioning error of magnetic head due to flow induced by disk rotation," IEEE Trans. Magn., Vol. 27, No, 6, pp. 5139-5141.

[9] Jiang, L., Miles,R.N.,1999, "A passive damper for the vibration modes of the head actuator in hard disk drives, " Journal of Sound and Vibration,Vol. 220, No 4,pp 683-694

[10] Blevins, R.D. 1977, "Flow-induced vibration", Van Nostrand Reinhold

[11] Naudascher, E., Rockwell. D., 1994, "Flow-induced vibrations: An engineering guide"

[12] Vickery, B.J., Davenport, A.G.,1967, "A comparison of theoretical and experimental determination of the response of elastic structures to turbulent flow", Symposium wind effects on buildings and structures, Ottawa, Canada.

[13]Chen, S. S., Wambsganns, M. W., 1972, "Parallel flow induced vibration of fuel rods," Nuclear Engineering Design, Vol. 18, pp 253-278

Disk speed (rpm)	6600	6900	7200	7500	7800	8100	8400	8700
Reduction (%)	15.9	4.4	0.4	4.8	10.37	15.8	15.6	18.4
Disk speed (rpm)	9000	9300	9600	9900	10200	10500	10800	11100
Reduction (%)	20.0	20.8	19.6	21.9	20.7	22.8	23.6	23.8

Table 1 Percentage reduction of $\hat{s}$ from the conventional cover to cover 2

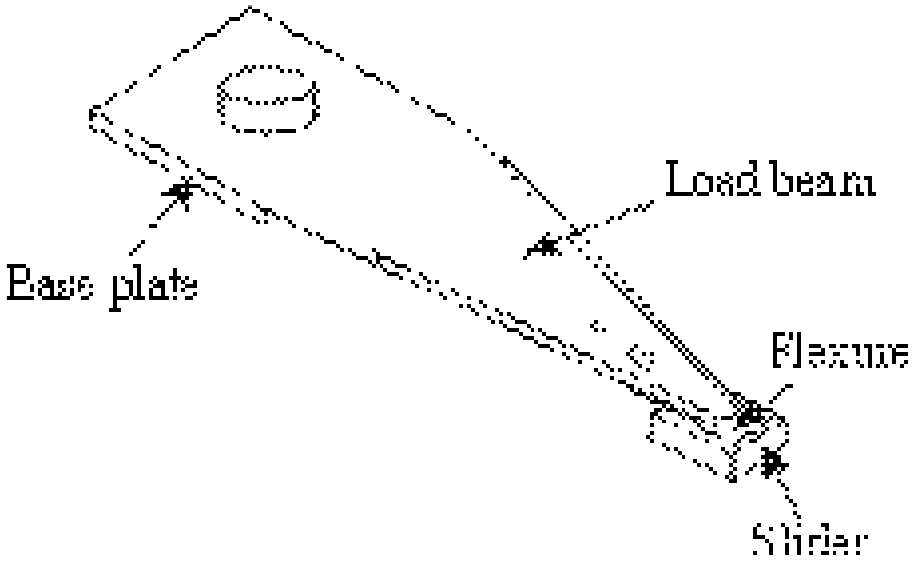

Fig. 1 Head gimbal assembly components

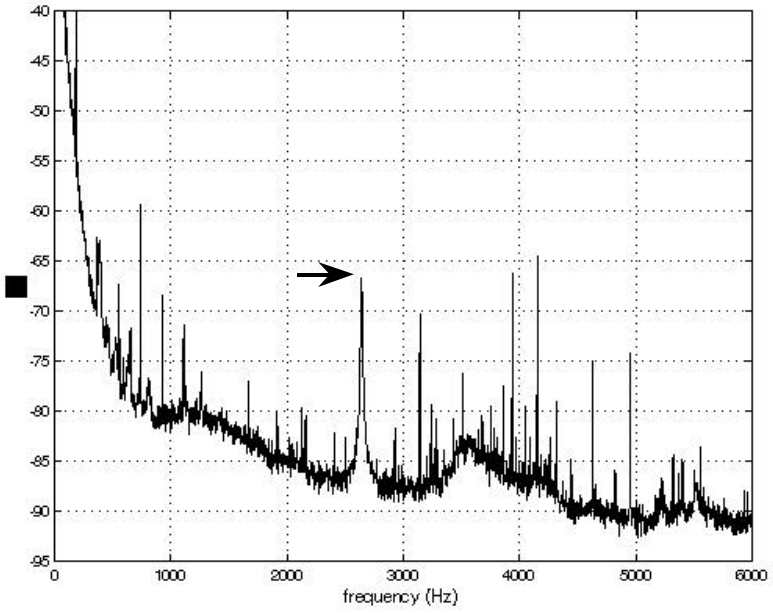

Fig. 2 PSD of radial slider displacement (Rs :32 mm, disk speed :11100 rpm)

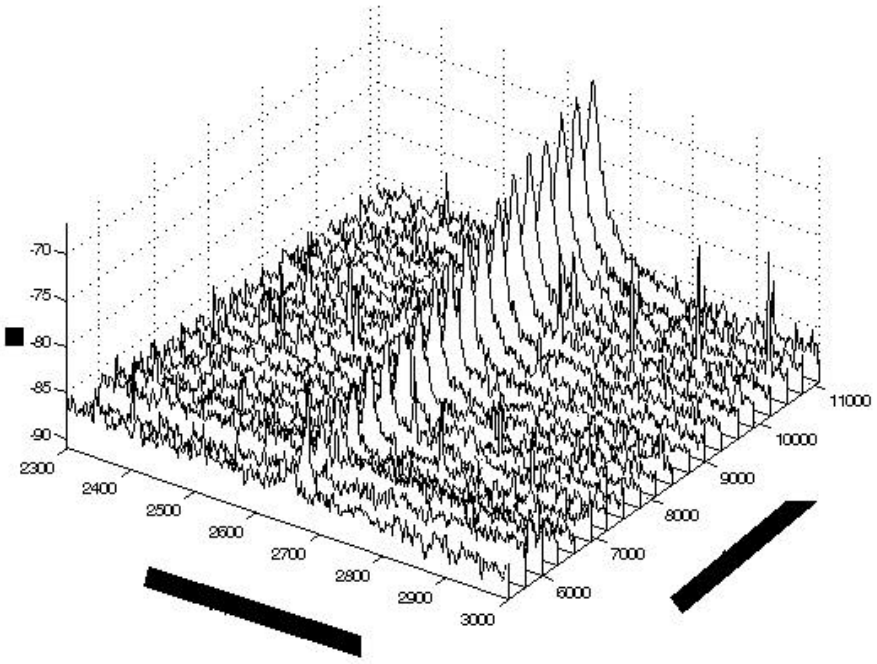

Fig. 3 PSD of slider displacement with disk speed.

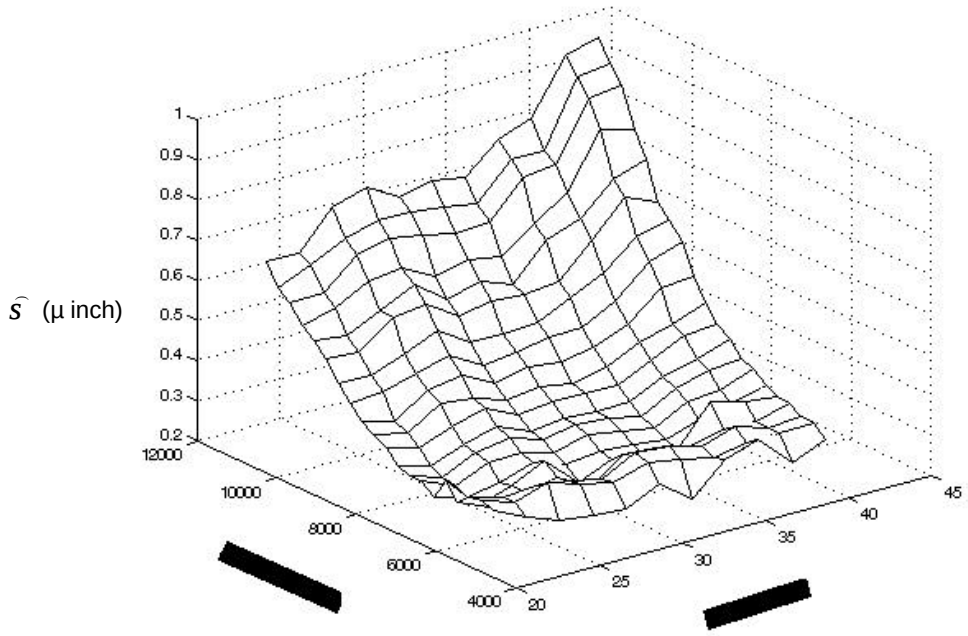

Fig. 4 $\hat{s}$ with disk speed and slider position

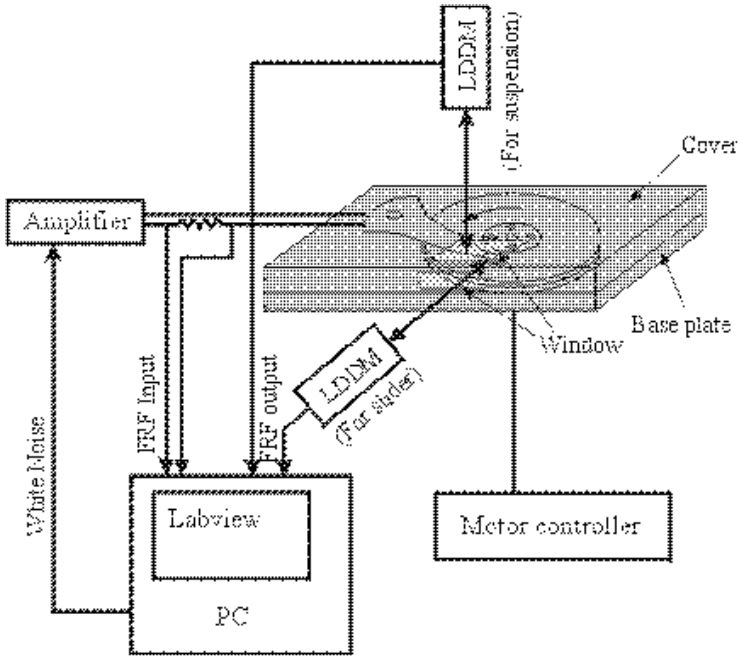

Fig. 5 Schematic of experimental setup for modal analysis of HGA

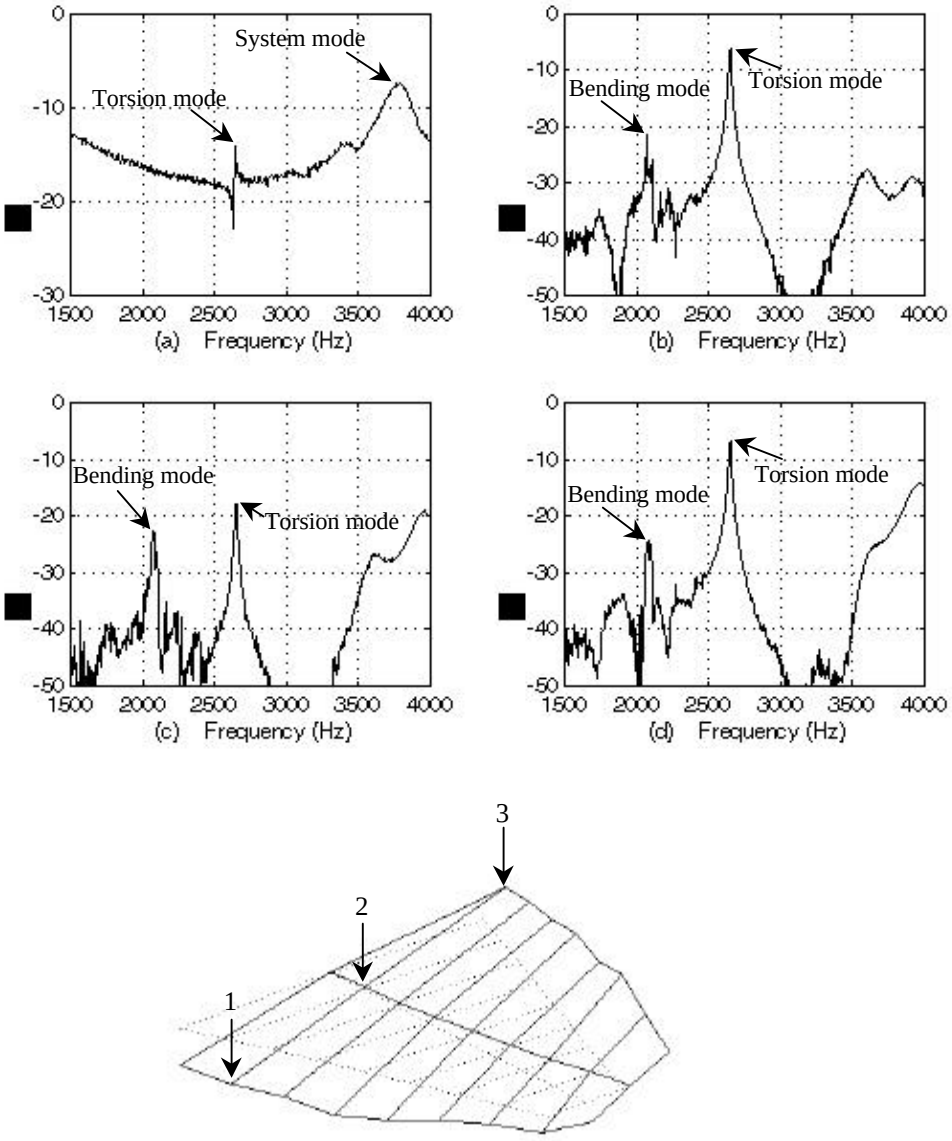

Fig. 6 Modal analysis results of HGA.

(a) Frequency response of radial slider displacement

(b) Frequency response of vertical load beam displacement (at point 1)

(c) Frequency response of vertical load beam displacement (at point 2)

(d) Frequency response of vertical load beam displacement (at point 3)

(e) Experimental mode shape of HGA at first torsional frequency

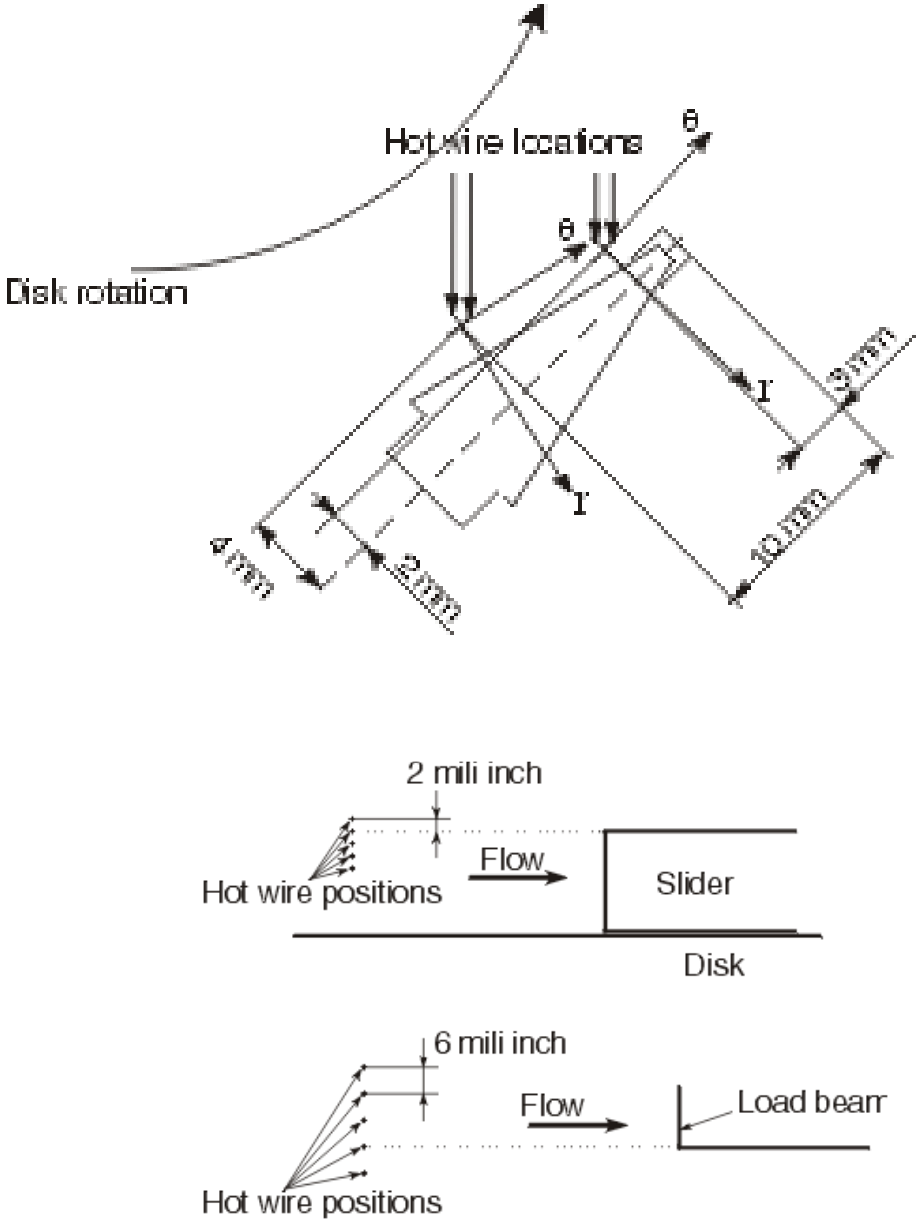

Fig. 7 Hot wire locations for measuring the flow upstream of suspension and slider

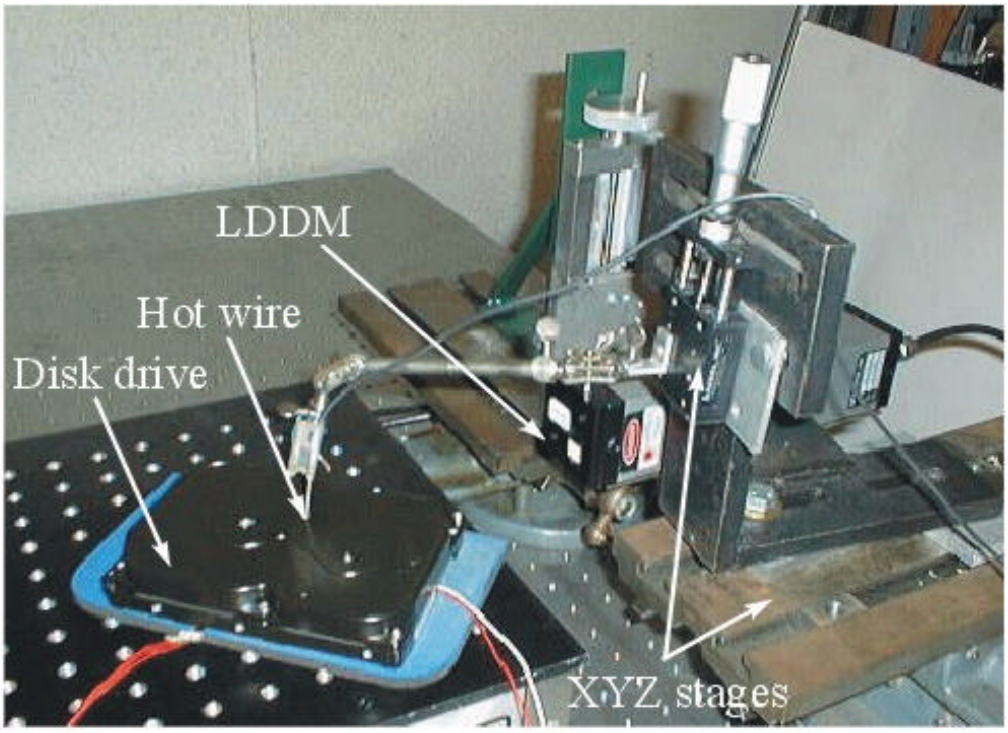

Fig. 8 Experimental setup for hot wire measurement

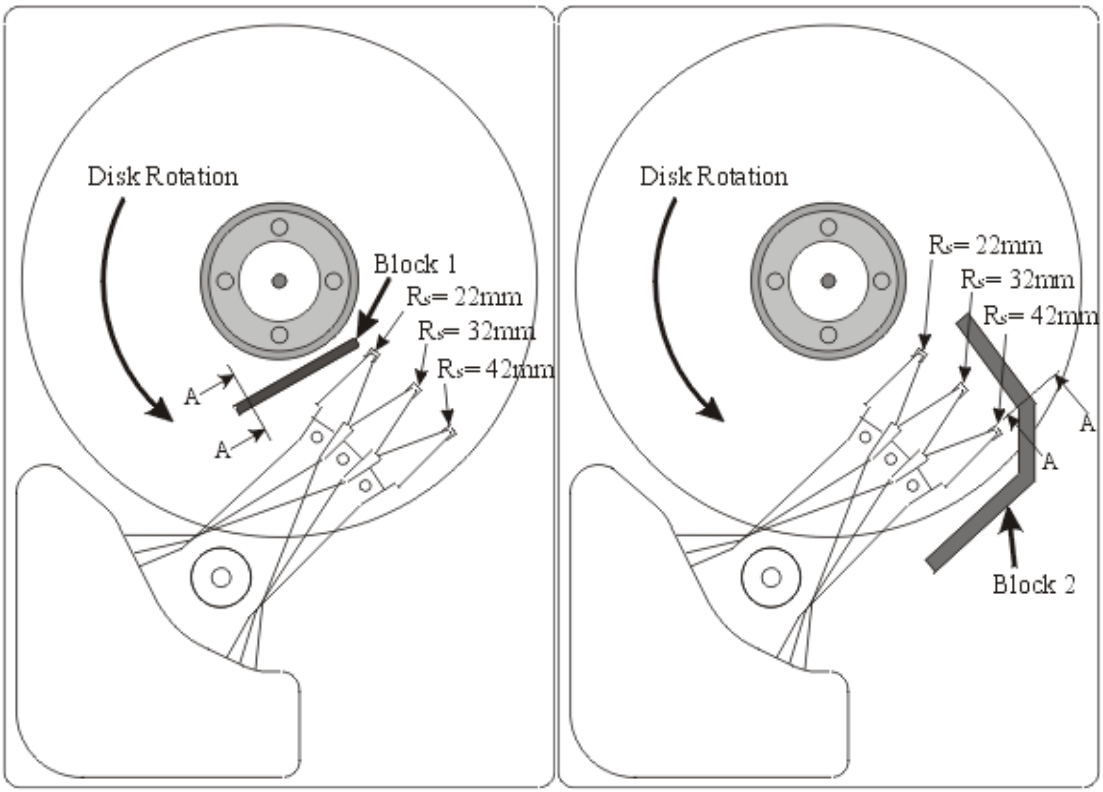

(a) (b)

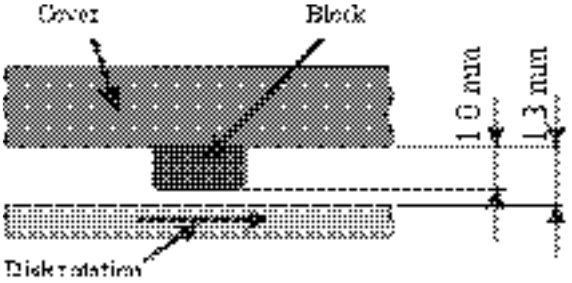

(c)

Fig. 9 Geometry of Cover 1 and Cover 2
(a) Cover 1, (b) Cover 2, (c) Section A-A

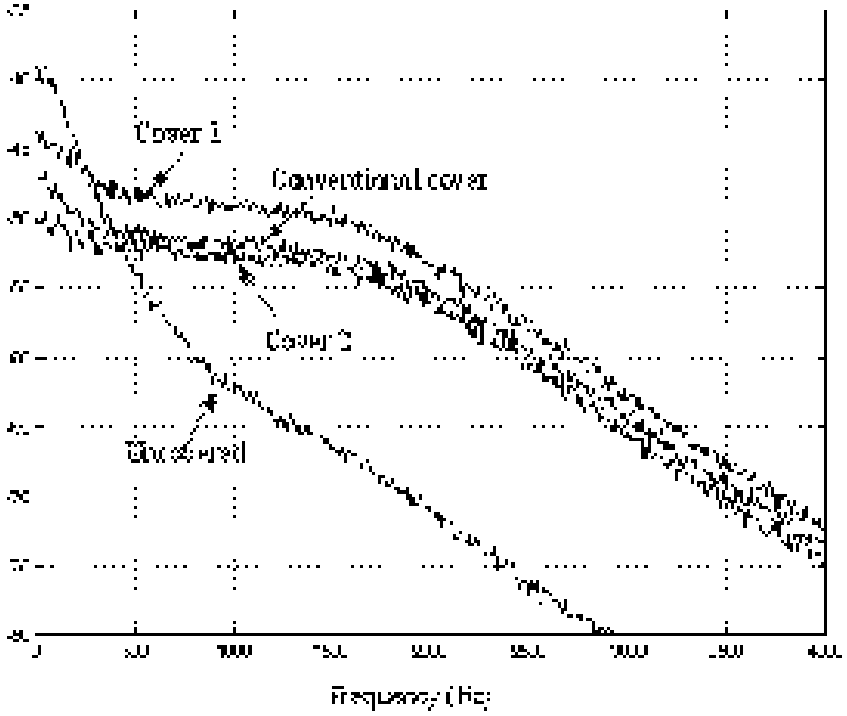

Fig. 10 Comparison of flow fluctuation
(upstream of suspension, radial direction, disk speed: 11100 rpm)

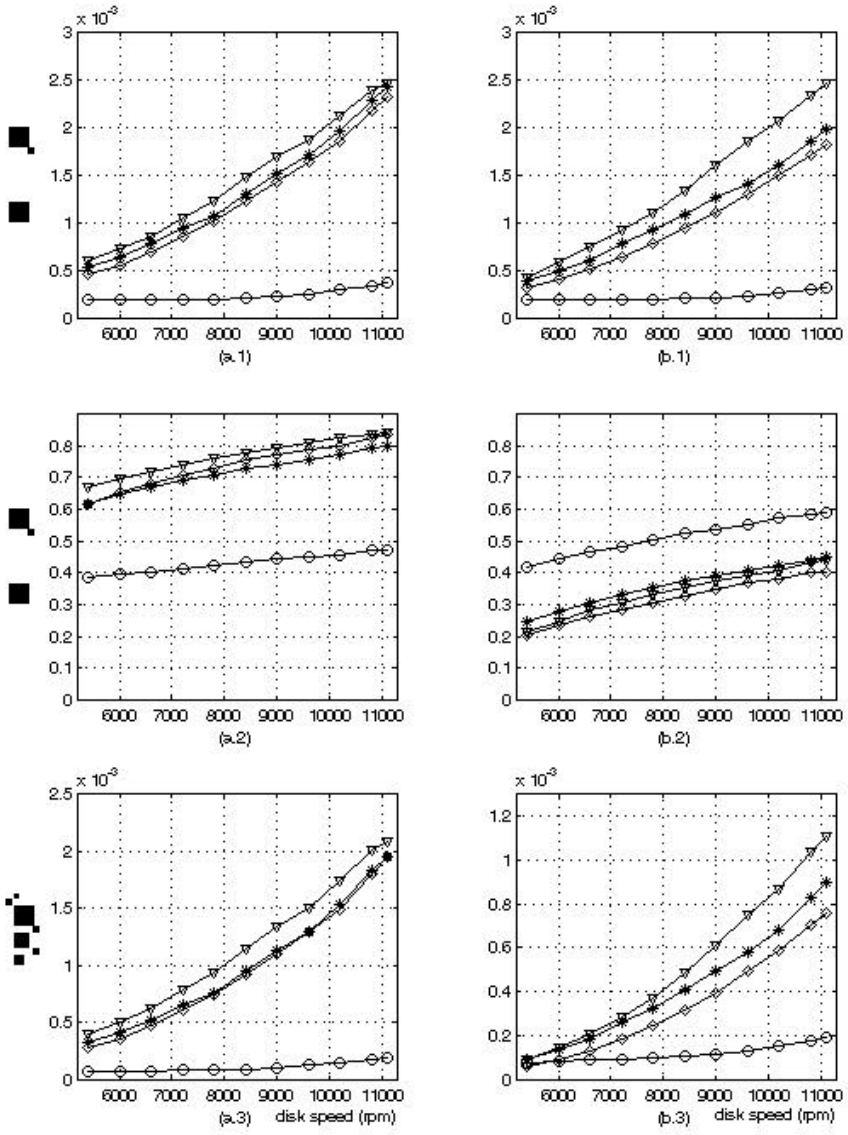

Fig. 11 Comparison of the voltage from hot wire anemometer with different cover. (upstream of load beam, averaged over 5 points in height from the disk, R_s = 32mm)

(a.1) v' in tangential direction in $\ddot{A}f$ (b.1) v' in radial direction in $\ddot{A}f$

(a.2) $\overline{v}$ in tangential direction (b.2) $\overline{v}$ in radial direction

(a.3) $\overline{v} \cdot v'$ in tangential direction (b.3) $\overline{v} \cdot v'$ in radial direction

$\ddot{A}f$: 2550 ~ 2750 Hz, $\overline{v}$: mean velocity, v' : fluctuating velocity

∇ : Cover 1, $\ast$: Conventional cover,

$\Diamond$: Cover 2, ï : Uncovered

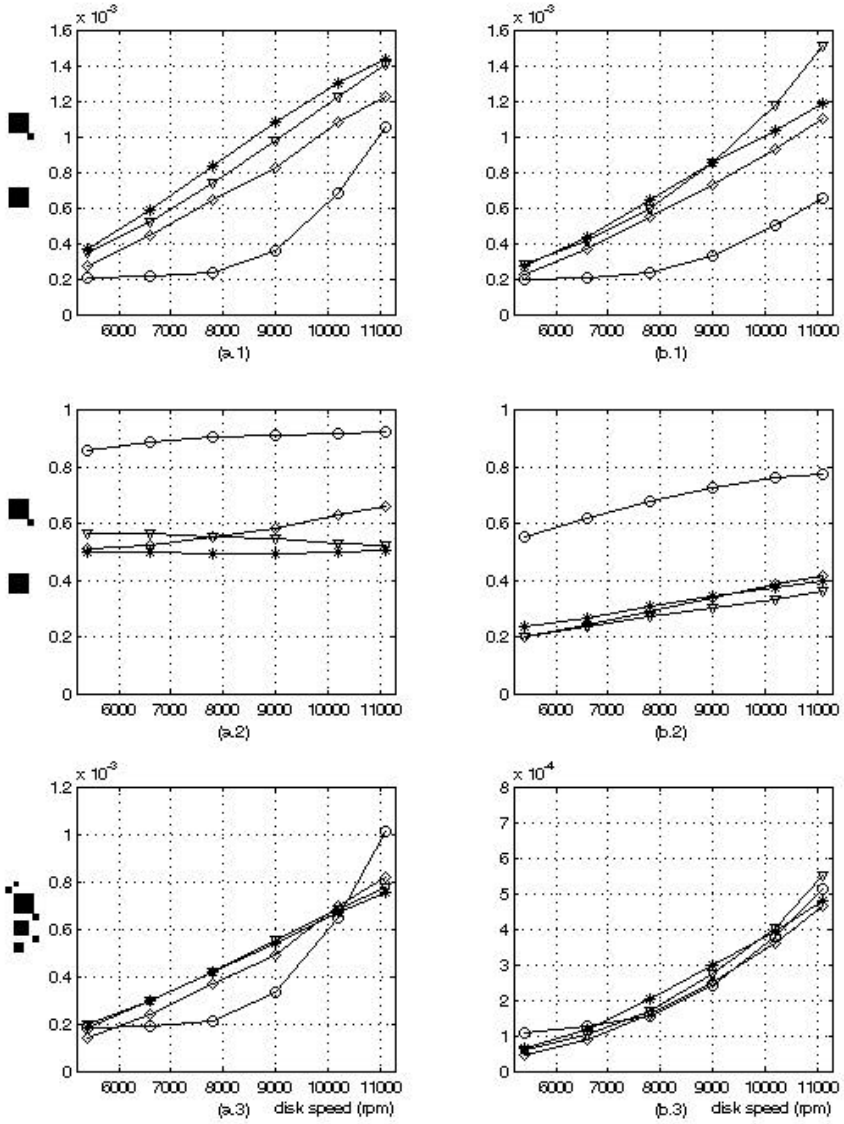

Fig. 12 Comparison of the voltage from hot wire anemometer with different cover. (upstream of slider, averaged over 5 points in height from the disk, R_s = 32mm)

(a.1) v' in tangential direction in $\ddot{A}f$ (b.1) v' in radial direction in $\ddot{A}f$

(a.2) $\bar{v}$ in tangential direction (b.2) $\bar{v}$ in radial direction

(a.3) $\bar{v} \cdot v'$ in tangential direction (b.3) $\bar{v} \cdot v'$ in radial direction

$\ddot{A}f$: 2550 ~ 2750 Hz, $\bar{v}$: mean velocity, v' : fluctuating velocity

∇ : Cover 1, $\ast$: Conventional cover,

$\Diamond$: Cover 2, ï : Uncovered

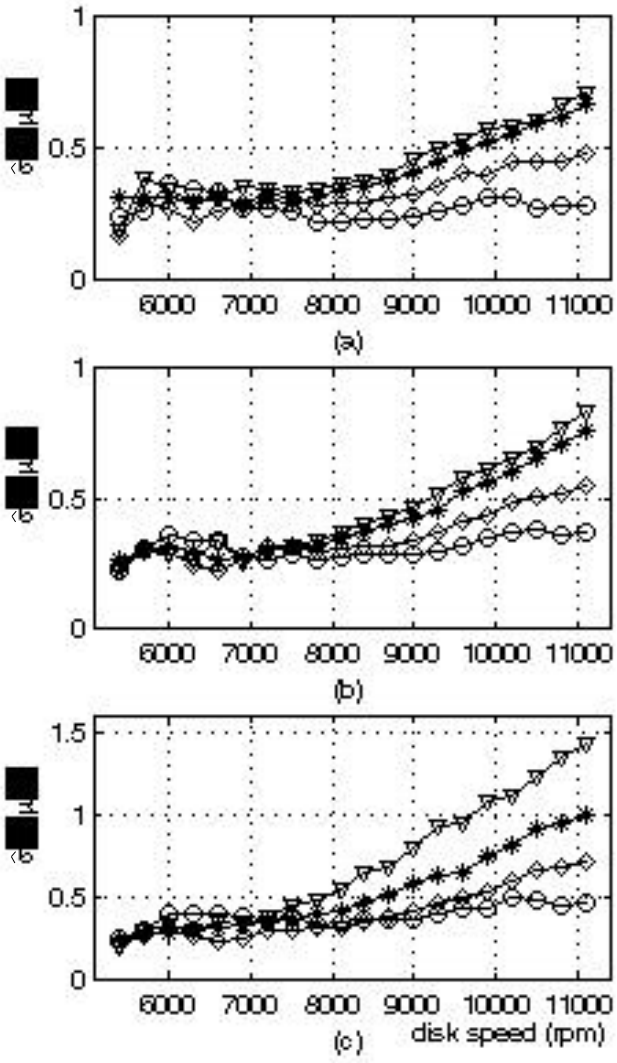

Fig. 13 Comparison of slider vibration $\hat{s}$ (μ inch)
∇ : Cover 1, ✳ : Conventional cover,
◊ : Cover 2, ï : Uncovered
(a) R_s = 22mm, (b) R_s = 32mm (c) R_s = 42mm

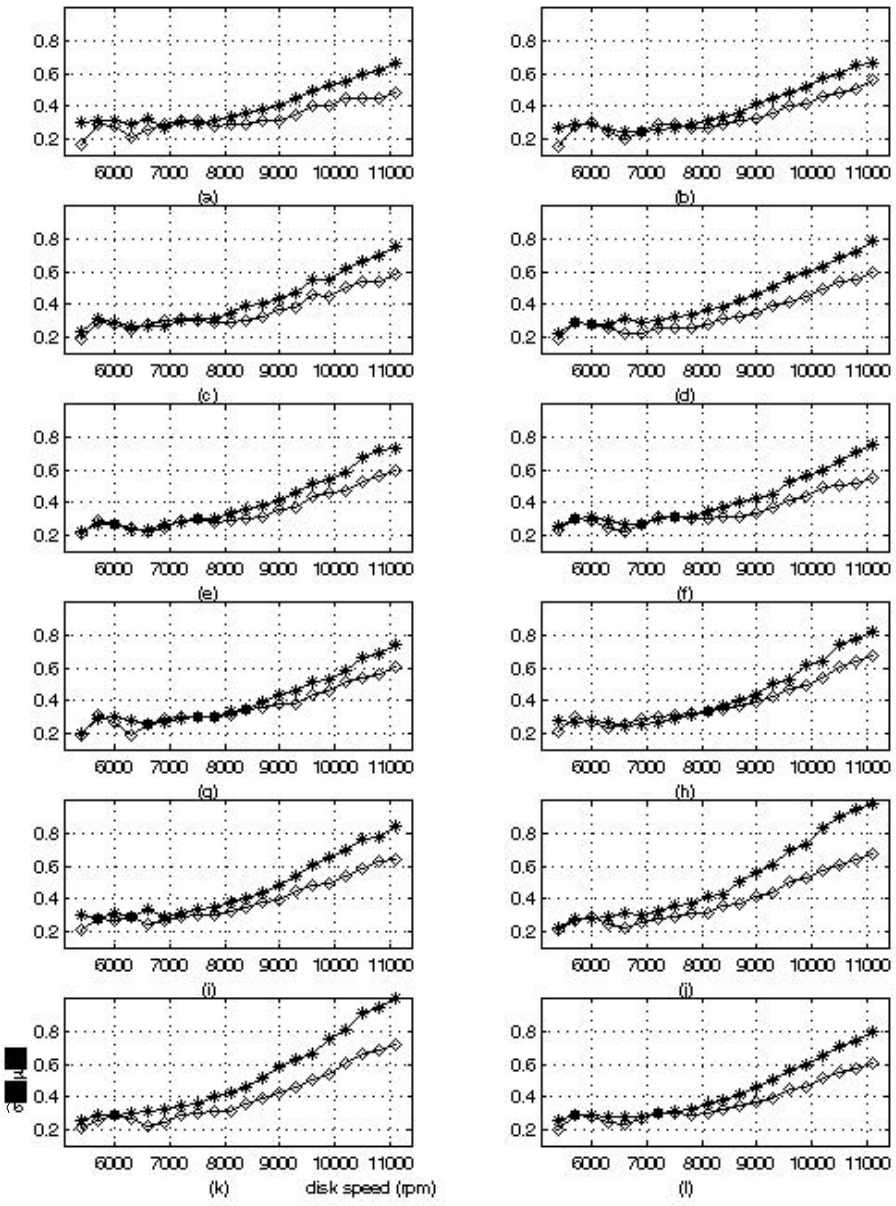

Fig. 14 Comparison of slider vibration in 1st torsional mode of suspension $\hat{s}$ (μ inch)
✳ : with conventional cover, ◊ : with cover 2
(a) R_s = 22 mm, (b) R_s = 24 mm, (c) R_s = 26 mm, (d) R_s = 28 mm,
(e) R_s = 30 mm, (f) R_s = 32 mm, (g) R_s = 34 mm, (h) R_s = 36 mm,
(i) R_s = 38 mm, (j) R_s = 40 mm, (k) R_s = 42 mm, (l) averaged over R_s